

広島大学学術情報リポジトリ  
Hiroshima University Institutional Repository

|            |  |
|------------|--|
| Title      | Palaeo — Stress Analysis of the Tsuji Overturned Fold in the Sambagawa Belt                          |
| Author(s)  | SEKI, Sachiyo; HARA, Ikuo; SHIOTA, Tsugio  |
| Citation   | Journal of science of the Hiroshima University. Series C, Geology and mineralogy , 9 (4) : 697 - 704 |
| Issue Date | 1993-07-30   |
| DOI        |  |
| Self DOI   | <a href="https://doi.org/10.15027/53128">10.15027/53128</a>  |
| URL        | <a href="https://ir.lib.hiroshima-u.ac.jp/00053128">https://ir.lib.hiroshima-u.ac.jp/00053128</a>    |
| Right      |  |
| Relation   |  |



## Palaeo-Stress Analysis of the Tsuji Overturned Fold in the Sambagawa Belt

By

Sachiyo SEKI, Ikuo HARA and Tsugio SHIOTA

*with 11 Text-figures*

(Received, March 30, 1993)

Abstract: Quartz microtextures of the Tsuji nappe with the Tsuji overturned fold in the Sambagawa belt, eastern Shikoku, have been analyzed to understand the movement picture of the Sambagawa schists which were exhumed into shallower tectonic position. The stress picture related to the formation of the Tsuji overturned fold has been clarified from deformation lamellae in quartz.

### Contents

- I. Introduction
- II. Description of quartz microtextures and palaeo-stress analysis
  - A. Tsuji stage
  - B. Ozu stage
- References

### I. Introduction

The geological structure of the Sambagawa schists in Shikoku is characterized by nappes produced throughout the three different deformations, pre-Ozu phase pile nappes, Tsuji stage pile nappes of the Ozu phase and Ozu stage pile nappes of the Ozu phase: The pre-Ozu phase pile nappes are the primary structure which is explained

in term of two way streets model (cf. Suppe,1972) such as the coupling of the exhuming units (=previously subcreted units) with the newly subcreted unit and appears to have been produced at the depth of larger than ca.4kb (Hara et al.,1992; Hara, 1993). This primary structure is a pile nappe structure consisting of the Saruta unit (Saruta nappe II and I), Fuyunose unit (Fuyunose nappe), Sogauchi unit [Sogauchi nappe containing the

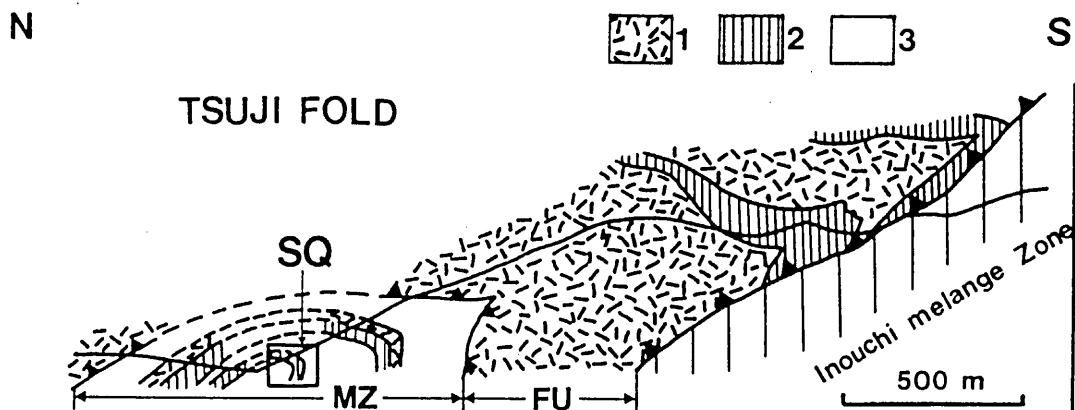


Fig. 1. Geological profile of the Tsuji nappe with the Tsuji overturned fold of the Tsuji district [compiled from the data of Shiota (1981), Hara et al.(1992) and the present authors].  
FU: Fuyunose unit (Tsuji basic schist), MZ: mixing zone, SQ: siliceous schist in which quartz microtextures have been studied in this paper, 1: basic schist, 2: siliceous schist, 3: pelitic schist

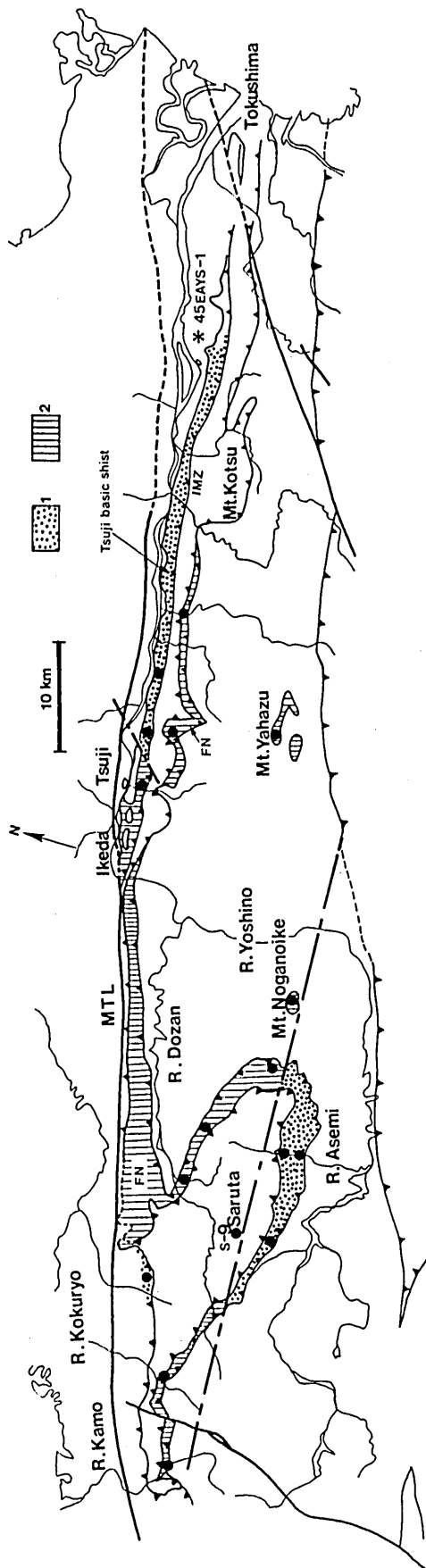


Fig. 2. Distribution of the Fuyunose unit in central-eastern Shikoku and its division based on the types of retrograde growth path of amphibole in hematite-bearing basic schist.

1: crossite-barroisite-winchite-actinolite path zone, 2: crossite-winchite-actinolite path zone.

FN: Fuyunose nappe, IMZ: Inouchi melange zone, solid circles: localities of the field data, S-9 and 45EAY-1: localities of the borehole data.

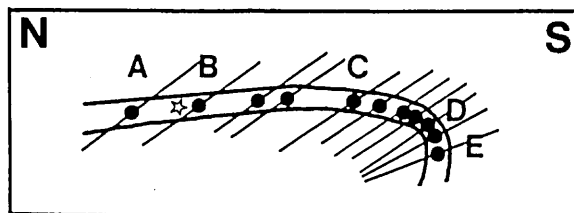


Fig. 3. Localities of samples with (solid circles) and without (open star) T-direction and orientation of T-direction plotted on a profile of the Tsuji overturned fold for the siliceous schist shown in Fig. 1. A, B, C, D and E: localities of samples for the data of Figs. 4, 5, 6, 7, 9 and 10. For fuller explanation see the Text.

Myoga - Sasagamine - Sogauchi - Toyosaka subunit (ST subunit), Kuma - Aguigawa - Takayabu - Kainayama - Kashidaira subunit (KAT subunit) and Nakayama - Nekosako - Okuoha - Mibuchi subunit (NOM subunit) and Oboke unit (Oboke nappe II and I) in descending order of structural level, which coincides with the younging order of subcretion. The Ozu phase pile nappes are the secondary structure which consists of nappes produced by the collapse of the primary structure in the shallow depth of less than ca.4kb and by the deformation probably referred to the horizontal ductile extension of the shallow part of accretionary wedge after Platt (1987) (Hara, 1993). The secondary structure consists of the Inouchi melange zone and its overlying Tsuji nappe in eastern Shikoku, Ojoi melange zone in central Shikoku and Terano-Isozu nappe and Saredani-Kabayama-Izushi nappe in western Shikoku. The Inouchi melange zone and Ojoi melange zone are of the Tsuji stage and remaining others are of the Ozu stage. The Tsuji nappe as the secondary structure is characterized by an overturned fold with southward closure (Tsuji overturned fold) (Fig. 1) (Shiota, 1980; Hara et al., 1992). Microtextures of quartz such as shape fabric, c-axis fabric and deformation lamellae and pressure shadows of the Tsuji overturned fold in the Tsuji district will be described and discussed in this paper, clarifying palaeo-stress and movement picture related to the formation of this fold and the Tsuji nappe.

#### Acknowledgements

The authors' works have been partly supported by the

Grant in Aid for Scientific Researches of the Ministry of Education of Japan.

## II. Description of Quartz Microtextures and Palaeo—Stress Analysis

### A. Tsuji Stage

The Inouchi melange zone and the lower part of the Tsuji nappe are the mixing zones of the Saruta unit (biotite zone schists) and Fuyunose unit (garnet zone schists) (Hara et al., 1992; Shiota et al., in preparation).

Fig. 1 illustrates a profile of the Tsuji overturned fold overlying the Inouchi melange zone. The Tsuji fold consists of two parts, mixing zone in the lower part and Fuyunose unit in the upper part. The Fuyunose unit of the upper part consists mainly of basic schist (Tsuji basic schist) of great thickness and extent (Fig. 2). Thus the Tsuji nappe appears to have initially been a member of the Inouchi melange zone and to be a secondary nappe produced in the upper part of the initial Inouchi melange zone. The retrograde growth history of amphibole in hematite-bearing basic schist involved in the fold belongs to three types after Hara et al. (1988, 1990), glaucophane—crossite—winchite—actinolite path and glaucophane—crossite—barroisite—winchite—actinolite path for the Fuyunose unit and hornblende—barroisite—actinolite path for the Saruta unit (Fig. 2) (Hara et al., 1992). But the basic schist of the mixing zone (lower part) involved in the fold of the Tsuji district shows the glaucophane—crossite—barroisite—winchite—actinolite path for the Fuyunose unit, while the Tsuji basic schist (upper part) shows as a whole the glaucophane—crossite—winchite—actinolite path, showing that the latter path of the Tsuji basic schist is in direct contact with the hornblende—barroisite—actinolite path in the mixing zone (Hara et al., 1992). The Tsuji basic schist is developed with great thickness and extent from the Tsuji district to the Kamojima district (Fig. 2). It is divided into two zones with reference to retrograde growth history of amphibole in hematite-bearing basic schist, crossite—winchite—actinolite path zone and crossite—barroisite—winchite—actinolite path zone, as shown in Fig. 2. The latter path zone is developed in great thickness in the Kamojima district, though that is almost absent in the Tsuji district, being developed only as small lenses in the mixing zone, (Hara et al., 1992). Thus it has been said that, just after the formation (Tsuji stage deformation) of the mixing zone with the Tsuji basic schist and of the Inouchi melange zone, the Tsuji folding occurred with an overturned fashion.

The W—B boundary between the crossite—winchite—actinolite path zone and the crossite—barroisite—winchite—actinolite path zone in the Tsuji basic schist (Fuyunose unit) is placed just on the east of the Tsuji district, as shown in Fig. 2 (Hara et al., 1992). The Fuyunose unit of the primary structure in eastern Shikoku, which underlies the Inouchi melange zone, is found only in some localities, though it is developed in great extent in central Shikoku, as shown in Fig. 2. This figure also illustrates the locality of the W—B boundary in the Fuyunose unit of the primary struc-

ture. The locality of the W—B boundary of the Tsuji basic schist is away by great distance from that of the Fuyunose unit of the primary structure. From this fact it has been assumed by Hara et al. (1992) that the Tsuji basic schist, together with the Inouchi melange zone schists, was displaced toward the north from the Fuyunose unit of the primary structure during the Tsuji stage.

### B. Ozu Stage

Microtextures of quartz of the Tsuji fold in the Tsuji district was analyzed in a siliceous schist layer shown in Fig. 1. The Tsuji fold of this siliceous schist is well observed in a large outcrop along the River Yoshino just on the west of Minoda—oohashi. Fifteen specimens to analyze quartz microtextures were collected from selected positions on a cross section of the fold as shown in Fig. 3. Quartz fabric data of these specimens will be shown in the following paragraphs.

The preferred shape orientation of quartz in the fold was measured on thin sections (B—section) normal to the fold axis. Its data for the hinge are illustrated in Fig. 4, showing that the long axes of quartz grains are preferably oriented parallel to the axial plane, i.e. defining the axial plane schistosity of the Tsuji fold.

Analogous pattern of shape orientation was also found in some positions in the hinge zone and limbs. For example, Fig. 5 illustrates the shape orientation of quartz in a position on the limb. The direction of preferred orientation in this figure also defines the axial plane schistosity (T direction) of the Tsuji fold. However, quartz grains in some other positions are preferably oriented parallel or subparallel to the bedding schistosity (B direction) but not to the T direction, as shown in Fig. 6, or show such complicated shape orientation as illustrated in Fig. 7. In quartz grains with the complicated shape fabrics are observed processes in which the B direction fabric was modified into the T direction fabric, showing that their shape fabrics in some parts of a thin section are characterized only by the T direction maximum but these in some others remain still fairly strong B direction maximum. The orientation pattern of the T direction in the Tsuji fold is schematically shown by Fig. 3. It is clear that the T direction is comparable with the principal axis X of strain in buckle fold (cf. Hara & Shimamoto, 1984). As observed on the B—section from the hinge, quartz grains are preferably oriented normal to the bedding schistosity and parallel to the axial plane, showing the marked T direction maximum (Fig. 4). This figure also illustrates the shape fabric observed on thin section (C—section) parallel to the bedding schistosity: The long axes of quartz grains are preferably oriented parallel to the fold axis and their aspect ratios are essentially the same as these on the B—section. From Fig. 4, therefore, it would be said that many quartz grains in the hinge approximate to oblate shape with the shortest axis normal to the axial plane, showing their aspect ratios around 2.5. Fig. 6 also shows that quartz grains with the marked B direction maximum as observed on the B—section are strongly elongated parallel to mineral lineation (Lm) defined by preferred shape orientation of

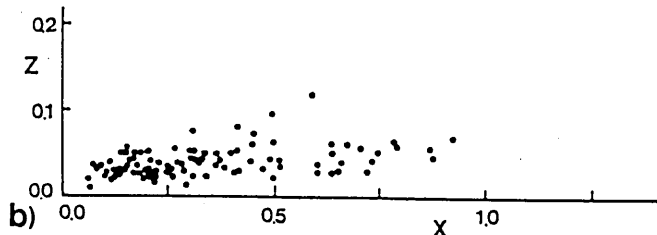
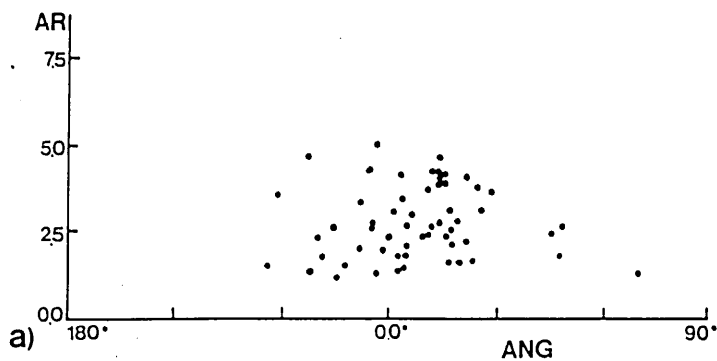
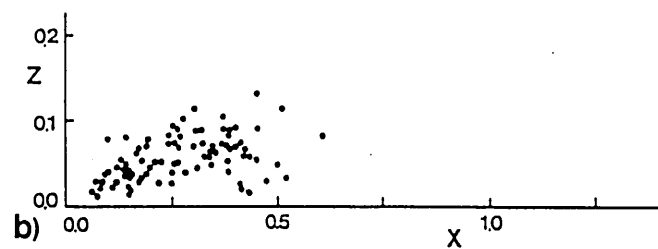
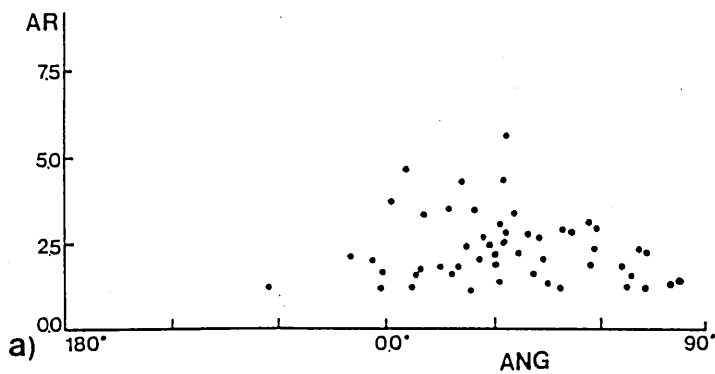
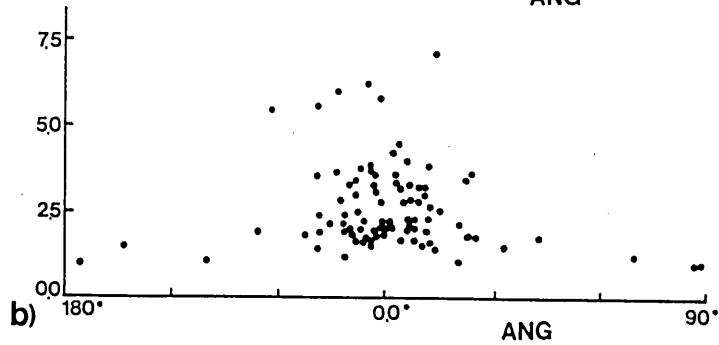
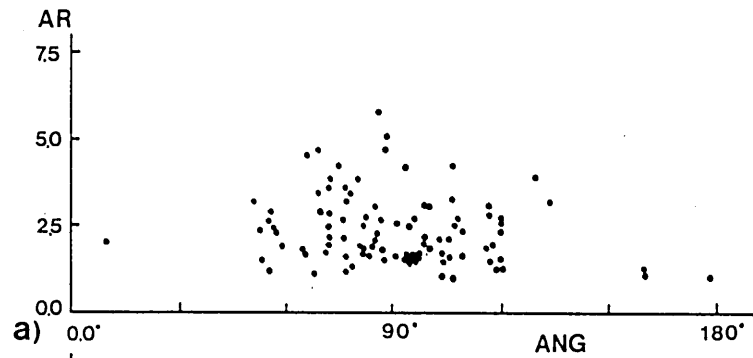


Fig. 4. Shape fabric data of quartz in the hinge (locality D).

a) data from B-section. AR: aspect ratio, ANG: angle between the bedding schistosity ( $Sb_1$ ) and the long axis of quartz ( $Lq$ ). b) data from C-section. ANG: angle between  $Lm$  and  $Lq$ . For fuller explanation see the Text.

Fig. 5. Shape fabric data of quartz on the limb (locality A).

a) data (T-direction maximum) from B-section. AR: aspect ratio, ANG: angle between  $Sb_1$  and  $Lq$ . b) data from A-section. X:  $Lq$ , Z: short axis of quartz ( $Ls$ ). For fuller explanation see the Text.

Fig. 6. Shape fabric data of quartz on the limb (locality B).

a) data (B-direction maximum) from B-section. AR: aspect ratio, ANG: angle between  $Sb_1$  and  $Lq$ . b) data from A-section. X:  $Lq$ , Z:  $Ls$ . For fuller explanation see the Text.

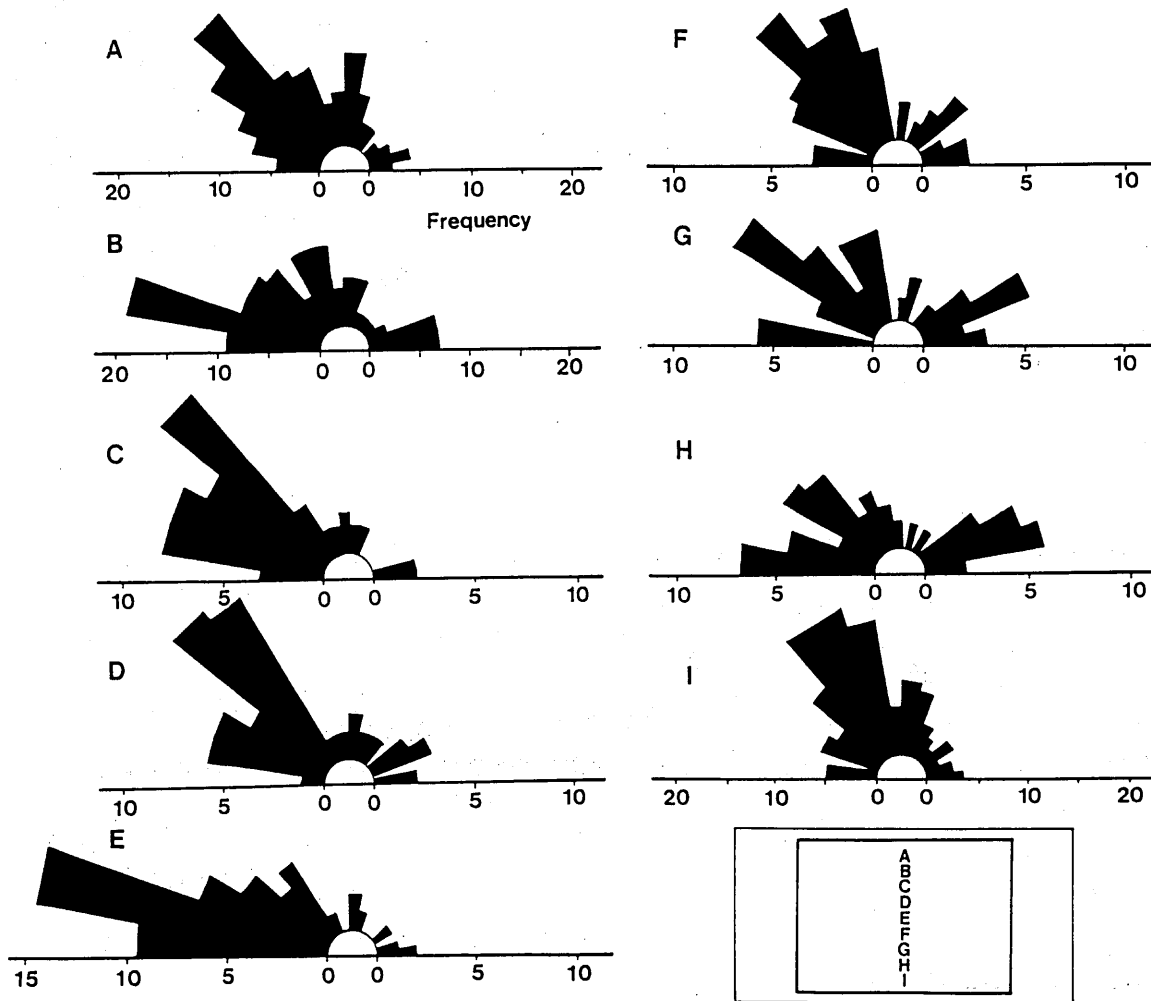


Fig. 7. Shape fabric data of quartz on the limb (locality C). The rose diagrams show great variation of Lq orientation in a B-section. A—I: localities of the data. Frequency is given by number of grain.

amphibole as observed on thin section (A-section) parallel to Lm and normal to the bedding schistosity. The aspect ratios for many quartz grains on the A-section are larger than 10 with the maximum aspect ratio of 35. Opaque minerals with euhedral-like and granular shapes are found in the specimen of Fig. 6, accompanying pressure shadows with feather quartz. Fig. 8 illustrates that quartz fringes forming pressure shadows is continuous with matrix quartz. As observed on the C-section, the elongation directions of pressure shadows and matrix quartz are parallel to Lm (Fig. 8). Large quartz grains, whose lengths parallel to Lm are between 5mm and 10mm, are frequently found in the specimens with the marked B direction maximum as shown in Fig. 6. Such large grains are not found in the specimens with only the T direction maximum (Fig. 5), showing that these are modified into small grains produced by dynamic recrystallization. Thus it would be said that the quartz shape fabric characterized by strong elongation parallel to Lm predated the Tsuji folding.

Fig. 9 illustrates the c-axis fabrics of quartz for two

specimens from the limb and for two specimens from the hinge. The c-axis fabric of Fig. 9-b is for the specimen with the marked B direction maximum (Fig. 6). It is characterized by type I crossed girdle. The c-axis fabric of Fig. 9-a is for the specimen with the marked T direction maximum (Fig. 5), which has been collected from the limb. It is characterized by a broad girdle normal to Lm. But in this diagram c-axes are highly dispersed. The fabric pattern of Fig. 9-b is quite harmonic with the strain picture assumed from the shape fabric and orientation pattern of the pressure shadows. The c-axis fabrics for the specimens from the hinge are illustrated in Fig. 9-c and d, showing that, in spite of preferred orientation of grain shapes (Fig. 4), c-axes are randomly dispersed on the diagrams. Thus it would be said that the degree of preferred orientation of c-axes decreases with progress of modification of the B direction shape fabric (fabric of pre-Tsuji folding phase) into the T direction shape fabric (fabric of Tsuji folding phase).

Some quartz grains in both limb and hinge have

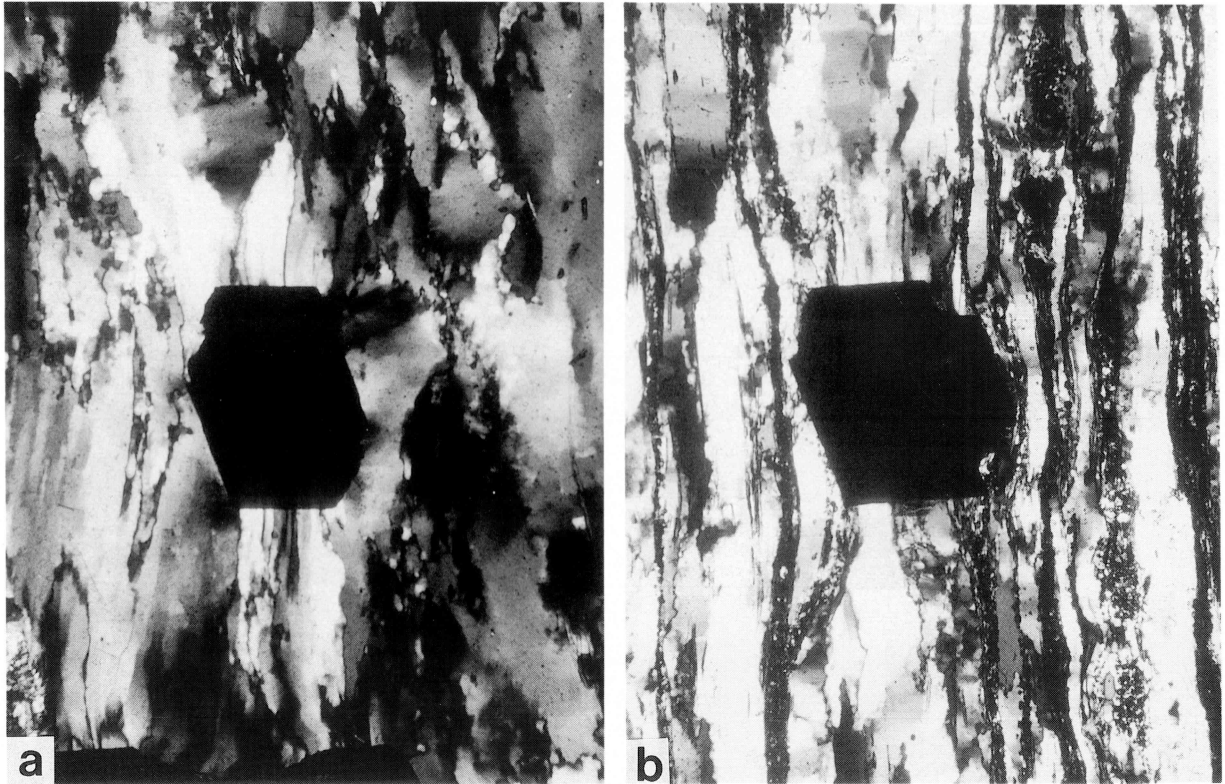


Fig. 8. Pressure shadows with quartz fringes as observed on C-section (a) and A-section (b).

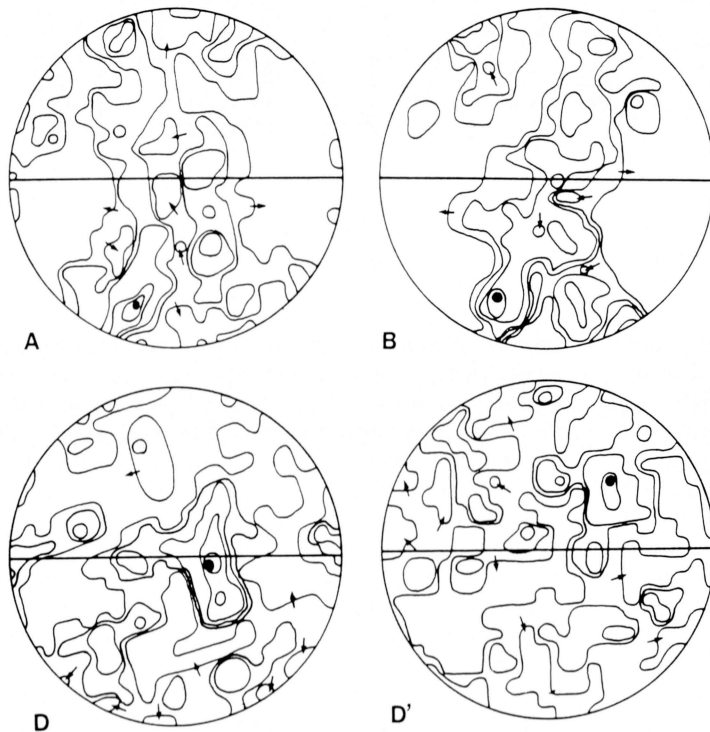


Fig. 9. *c*-axis fabrics of quartz for specimens from localities A, B and D. D and D': data for two specimens from the locality D. solid straight line:  $Sb_1$ , center of diagram: normal to the fold axis.

deformation lamellae. Fig. 10 illustrates the crystallographic location of these lamellae as measured as angle between c-axis and lamellae pole in individual grains, showing a marked maximum between 5° and 15°. From this figure it would be said that the lamellae are roughly referred to the type of subbasal I after Avelallemant and Carter (1971). Fig. 11 is the diagram showing the orientation pattern of a partial great circle between the c-axis (tail) and lamellae pole (arrow head) of individual grains. These diagrams are for the arrow method of the palaeo—stress analysis, in which the tail and the arrow head are closer to the compression axis and to the tension axis respectively (cf. Cater et al., 1964; Heard & Carter, 1968). The data for each diagram of Fig. 11 were measured and synthesized from three sections which are oriented normal to each other. The compressive stress axis and tensional stress axis assumed from these data are also plotted in this figure.

As is obvious in Fig. 9—c and d, c-axes of quartz grains in the hinge are randomly dispersed, showing no unique fabric pattern. Thus, the assumed orientation directions of the compressive stress axis and tensional stress axis are considered to be available. From Fig. 11, therefore, it would be said that the trajectories of the compressive stress axis and tensional stress axis

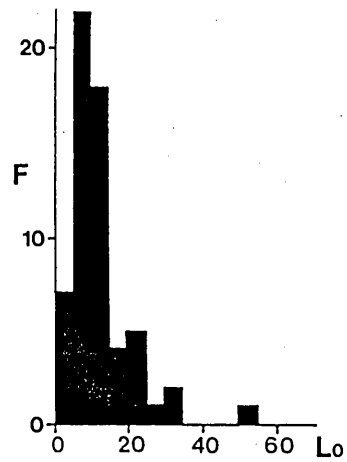


Fig. 10. Crystallographic location of deformation lamellae in quartz. Lo: angle between c-axis of grain hosting lamellae and pole to the lamellae, F: Frequency is given by number of grain.

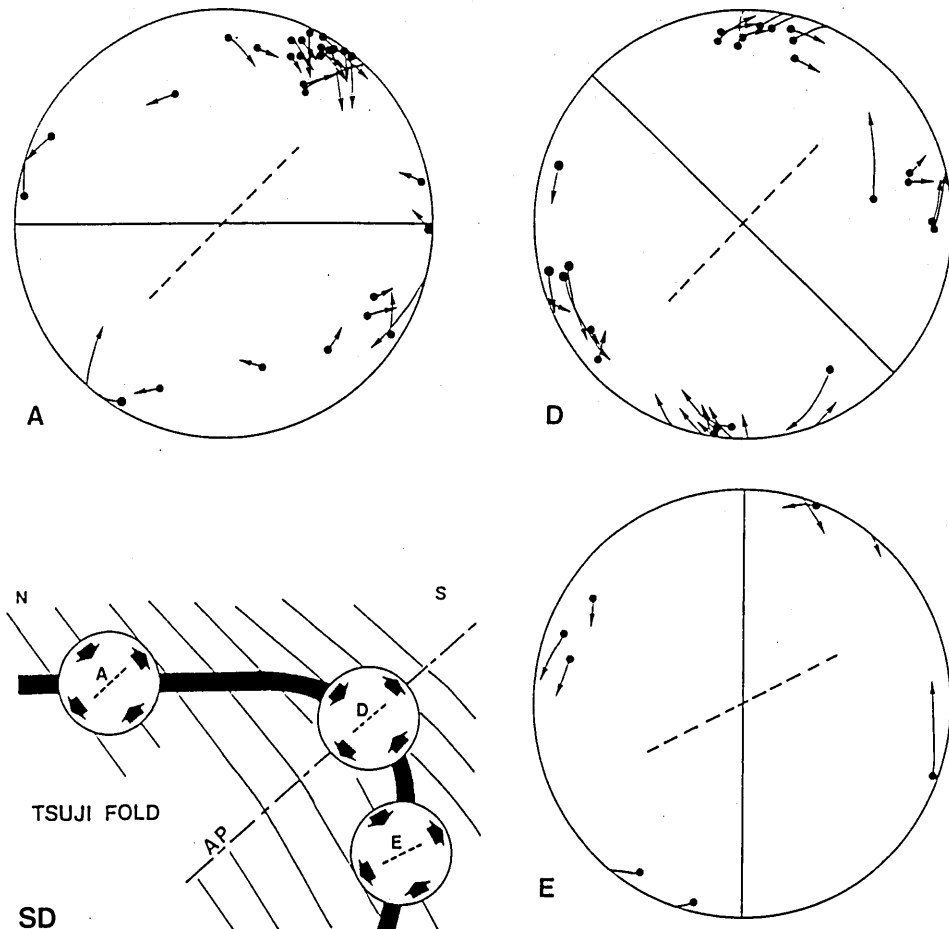


Fig. 11. Palaeo—stress analysis of the Tsuji fold based on deformation lamellae in quartz. arrow heads: lamellae pole, solid circles: c-axis of grain hosting lamellae, solid straight line:  $Sb_1$ , dashed line: T-direction, A, D and E: data for specimens from localities A, D and E respectively. SD: orientation of compressive stress axis and tensional stress axis assumed from the data A, D and E. solid lines: trajectory of compressive stress axis in the Tsuji fold, AP: axial plane of the Tsuji fold.



throughout the Tsuji fold are oriented normal to its axial plane and normal to its fold axis respectively. Such the stress picture assumed from the lamellar fabric must be for the Tsuji folding and is harmonic with the shape of the Tsuji fold which shows a southward clouse. Thus it would be assumed that the deformation related to the formation of the Tsuji fold and so Tsuji nappe was of a southward vergence. The stress picture for the deformation lamellae is not harmonic with the c-axis fabric on the limb (Fig. 9-b) and the orientation pattern of pressure shadows, showing that the latter types fabrics predated the Tsuji folding and were produced during the Tsuji stage deformation, which was responsible for the formation of mixing zone of garnet zone schists and biotite zone schists.

Sachiyo SEKI and Ikuo HARA

Department of Earth and Planetary Systems Science, Faculty of Science, Hiroshima University, Higashi-hiroshima, 724, Japan.

Tsugio SHIOTA

Division of Natural Sciences, Faculty of Integrated Arts and Sciences, Tokushima University, Tokushima, 770, Japan.

### References

- AveLallement, H.G. and Carter, N.L., 1971: Pressure dependence of quartz deformation lamellae orientation. *Am. Jour. Sci.* 270, 218–235.
- Carter, N.L. Christie, J.M. and Griggs, D.T., 1964: Experimental deformation and recrystallization of quartz. *Jour. Geol.* 72, 687–733.
- Hara, I., 1993: Some considerations on research history (1971–1992) of tectonics of the Chyugoku, Ryoke, Sambagawa and Chichibu belts. In *Hundred Years of Geology in Japan. Centennial Vol. Geol. Soc. Japan.* 202–212.
- Hara, I., Shiota, T., Takeda, K. and Hide, K., 1988: Tectonics of the Sambagawa Terrane. *Earth, Monthly*, 10, 372–378.
- Hara, I., Shiota, T., Takeda, K., Okamoto, K. and Hide, K., 1990: The Sambagawa Terrane. In Ichikawa et al. eds, *Pre-Cretaceous Terranes of Japan.* Publication of IGCP, 224, 137–163.
- Hara, I., Shiota, T., Hide, K., Kanai, K., Goto, M., Seki, S., Kaikiri, K., Takeda, K., Hayasaka, Y., Miyamoto, T., Sakurai, Y. and Ohotomo, Y., 1992: Tectonic evolution of the Sambagawa schists and its implications in convergent margin processes. *Jour. Sci. Hiroshima Univ. Ser. C*, 9, 495–595.
- Heard, H.C. and Carter, N.L., 1968: Experimentally induced 'natural' intragranular flow in quartz and quartzite. *Amer. Jour. Sci.* 266, 1–42.
- Platt, J.P., 1987: The uplift of high-pressure – low temperature metamorphic rocks. In Oxburgh E.R., Yardley B.W.D. and England P.C. eds, *Tectonic Setting of Regional Metamorphism.* The Royal Society, 87–103.
- Shiota, T., 1981: Structural, geological and petrological study of the Sambagawa crystalline schists of the Ikeda–Mikamo district, East Shikoku. *Jour. Gakugei, Tokushima Univ. (Nat. Sci.)*, 32, 29–65.
- Suppe, J., 1972: Interrelationships of high-pressure metamorphism, deformation and sedimentation in Franciscan tectonics, USA. 24th IGC, Section 3, 552–559.